

In vivo assessment of marine vs bovine origin collagen-based composite scaffolds promoting bone regeneration in a New Zealand rabbit model

Gabriela S. Diogo^{a,b}, María Permuy^{c,d}, Catarina F. Marques^{a,b}, Carmen G. Sotelo^e,
Ricardo I. Pérez-Martín^e, Julia Serra^{f,g}, Pio González^{f,g}, Fernando Munõz^{c,d},
Rogério P. Pirraco^{a,b}, Rui L. Reis^{a,b}, Tiago H. Silva^{a,b,*}

^a 3B's Research Group, I3Bs – Research Institute on Biomaterials, Biodegradables and Biomimetics, University of Minho, Headquarters of the European Institute of Excellence on Tissue Engineering and Regenerative Medicine, AvePark, Parque de Ciência e Tecnologia, Zona Industrial da Gandra, 4805-017 Barco, Guimarães, Portugal

^b ICVS/3B's - PT Government Associate Laboratory, Braga/Guimarães, Portugal

^c Dpto. Anatomía, Producción animal e Ciencias Clínicas Veterinarias, Universidade de Santiago de Compostela, Av Carvallo Calero s/n, 27002 Lugo, Spain

^d iBoneLab SL, Av da Coruña 500, 27003 Lugo, Spain

^e Instituto de Investigaciones Marinas (CSIC), Eduardo Cabello 6, 36208 Vigo, Spain

^f CINTECX, Universidade de Vigo, Grupo de Novos Materiais, 36310 Vigo, Spain

^g Galicia Sur Health Research Institute (IIS Galicia Sur), SERGAS-UVIGO, 36213 Vigo, Spain

ARTICLE INFO

Keywords:

Fish collagen

Apatite

Blue shark

Bone regeneration

New Zealand rabbit

Marine biomaterials

ABSTRACT

The ability of human tissues to self-repair is limited, which motivates the scientific community to explore new and better therapeutic approaches to tissue regeneration. The present manuscript provides a comparative study between a marine-based composite biomaterial, and another composed of well-established counterparts for bone tissue regeneration. Blue shark skin collagen was combined with bioapatite obtained from blue shark's teeth (mColl:BAP), while bovine collagen was combined with synthetic hydroxyapatite (bColl:Ap) to produce 3D composite scaffolds by freeze-drying. Collagens showed similar profiles, while apatite particles differed in their composition, being the marine bioapatite a fluoride-enriched ceramic.

The marine-sourced biomaterials presented higher porosities, improved mechanical properties, and slower degradation rates when compared to synthetic apatite-reinforced bovine collagen. The *in vivo* performance regarding bone tissue regeneration was evaluated in defects created in femoral condyles in New Zealand rabbits twelve weeks post-surgery. Micro-CT results showed that mColl:BAP implanted condyles had a slower degradation and an higher tissue formation ($17.9 \pm 6.9\%$) when compared with bColl:Ap implanted ones ($12.9 \pm 7.6\%$). The histomorphometry analysis provided supporting evidence, confirming the observed trend by quantifying $13.1 \pm 7.9\%$ of new tissue formation for mColl:BAP composites and $10.4 \pm 3.2\%$ for bColl:Ap composites, suggesting the potential use of marine biomaterials for bone regeneration.

1. Introduction

In the orthopedic field, allografts, artificial bone grafts and, particularly, autografts, are still the golden standard treatments for critical-size bone defects [1]. However, the limited availability of donor tissue, the site morbidity and, ultimately, the poor efficiency of these treatments have been touching the scientific community to investigate alternative routes [1,2]. In the practice of guided bone tissue

regeneration, clinicians often employ biomaterials as barriers to prevent the formation of fibrous tissue in the wound while enhancing the healing process [3]. Thus, many different tissue engineering (TE) approaches have been thought to improve bone regeneration, being the 3-dimensional (3D) structures the first option since they can recapitulate in a more realistically way the spatial microarchitecture of the native bone [4]. For that, customization by applying different materials composition and processing technologies have been explored to design 3D structures

* Corresponding author at: 3B's Research Group, I3Bs – Research Institute on Biomaterials, Biodegradables and Biomimetics, University of Minho, Headquarters of the European Institute of Excellence on Tissue Engineering and Regenerative Medicine, AvePark, Parque de Ciência e Tecnologia, Zona Industrial da Gandra, 4805-017 Barco, Guimarães, Portugal.

E-mail address: tiago.silva@i3bs.uminho.pt (T.H. Silva).

<https://doi.org/10.1016/j.bioadv.2024.213813>

Received 13 October 2023; Received in revised form 7 February 2024; Accepted 23 February 2024

Available online 26 February 2024

2772-9508/© 2024 The Authors. Published by Elsevier B.V. This is an open access article under the CC BY-NC-ND license (<http://creativecommons.org/licenses/by-nc-nd/4.0/>).

with appropriated mechanical, degradation, and biological properties to be used as templates for cell growth towards new tissue formation.

Polymeric materials, particularly, natural polymers have been gaining importance as a hopeful resource for bone tissue engineering applications, thanks to their availability and resemblance to the components of the native extracellular matrix in connective tissue [3]. Collagen-based solutions stand out as particularly promising biomaterials since they offer attractive biological cues that encourage cell and tissue integration *in vivo* with a reduced inflammatory response and, additionally, represent biodegradation and bioresorbability capabilities. Within the “collagen world”, mammalian origin collagens still occupy the leaders’ position. However, the risk of disease transmission to humans, as bovine spongiform encephalopathy (BSE), and the associated religious constraints together with ethical perspectives refraining the use of materials from mammal origin, have been questioning its use [5]. In this perspective and considering the growing need for collagen-based therapeutic approaches and the limited sources for safe collagen, the exploration of marine organisms has been increasing, from different fish species to other marine origin organisms like jellyfish, sponges and mollusks [6].

In vitro, the cytocompatibility of marine collagen-derived biomaterials has been assessed with different cell lines but also with stem cells and the results are promising [7,8]. Human mesenchymal stem cells cultured on tilapia collagen coated dishes revealed similar cytocompatibility results comparatively with porcine collagen coated dishes [9]. Collagen from blue shark *Prionace glauca* was used to produce 3D composite scaffolds and the results exhibited better cytocompatibility when compared with bovine collagen scaffolds [8]. Despite the exponential increase of marine origin studies reported in the last years, only a few *in vivo* studies have been stated [10–12]. In general, fish derived collagens have lower denaturation temperatures, which may have a negative impact when tested *in vivo* due to its fast biodegradation, eventually contributing to the small amount of *in vivo* works arising from the application of marine origin-materials. In this regard, many different techniques of structures manufacturing are commonly used to increase collagen stability. Hassanbhai et al. did show a higher denaturation temperature of electrospun tilapia collagen membranes when cross-linked with glutaraldehyde, in comparison with a commercial available solution, Bio-Gide®, a porcine collagen membrane [13]. The membranes were not cytotoxic and even with its faster *in vivo* degradation, the immune response was similar with that of porcine. Also, Nagai et al. revealed outstanding results with scaffolds made of crosslinked salmon collagen, showing a similar microarchitecture and cell proliferation rate comparatively to bovine collagen scaffolds [14].

Alternatively, marine collagens have been combined with robust materials such as ceramics, improving their mechanical properties and stability. In the field of bone regeneration, this composite promotes the formation of new bone by releasing calcium and phosphate ions, thus fostering the mineralization process [15].

Bone grafts of natural origin obtained from non-human species, including marine origin by-products, has received much attention in last decades, particularly shark tooth from 2 commercial species, *Isurus oxyrinchus* and *Prionace glauca* [16,17]. Shark tooth is gaining increasing recognition as a promising, eco-friendly source of bioapatites, since it is an abundant by-product from fishing, being environmentally sustainable. The incorporation of the marine bioapatite particles into a marine collagen matrix can be a perfect combination to ensure good performance in hard tissue applications.

In our previous work [18] it was tested the *in vitro* potential of scaffolds made of blue shark collagen combined with bioapatite granules obtained from the teeth of the same species. The present work was designed to validate the *in vivo* potential of using such scaffolds for the regeneration of bone defects and, to compare an entire marine-based biomaterial with one composed of bovine collagen and synthesized hydroxyapatite when implanted *in vivo*. The motivation for selecting bovine collagen and synthetic apatite, as comparable materials, is based

on a market assessment, whereas it was found that most of the collagen and apatite products already in commercialization have bovine and synthetic origin, respectively. Bovine collagen is highly available being mostly obtained from bovine discards, as hides, tendons and bones, by-products of meat production [19,20]. Synthetic hydroxyapatite is often used for biomedical applications, mostly because of its predictable homogeneous composition matching the mineral component of bone tissue, and its low-obtaining costs. Bone defects were created in rabbit models and the biomaterials were implanted, evaluating new bone tissue formation twelve weeks post-implantation, namely addressing the percentage of bone-like tissue formation by two different methodologies, micro-CT and histomorphometry.

2. Materials and methods

2.1. Materials origin

Skin and teeth of blue sharks were obtained from Centro Tecnológico del Mar (CETMAR, Vigo, Spain) and COPEMAR SA (fishing company, Spain). Collagen was isolated from blue shark (*Prionace glauca* (PG)) and bovine skin. Biological apatite (BAp) was obtained from the teeth of *Prionace glauca* and *Isurus oxyrinchus* and commercial apatite (Ap) was obtained from Plasma Biotol Ltd. (Derbyshire, UK).

2.2. Collagen extraction procedure

Marine collagen (mColl) and bovine (bColl) origin collagen were extracted through a very well established acid solubilization method [21]. The process was divided in three main steps: processing of raw materials, which includes size reduction and cleaning followed by pre-treatment with an alkaline solution (0.1 M NaOH, during 24 h at 4 °C) to remove non-collagenous proteins; the second step was the extraction of collagen with 1 M acetic acid solution (1:10 (w:v), for 72 h at 4 °C). The extracted collagen was precipitated (overnight) with 2 M NaCl and separated by centrifugation. For purification, the retrieved collagen was resolubilized in acetic acid and subjected to a dialysis process with successive decreasing concentrations of acetic acid, for 8 days, to remove any residual contaminations. The final collagen was then freeze-dried.

2.3. Collagen characterization

2.3.1. Amino acid profile

To characterize the extracted marine collagen (mColl) and bovine collagen (bColl), the amino acid composition was quantitatively assessed by using a Biochrom 30 (Biochrom Ltd., Cambridge, UK) at Centro de Investigaciones Biológicas of the Spanish National Research Council (CSIC), in Madrid (Spain). After extraction, both origin collagens were hydrolyzed and separated through a cation-exchange resin column accordingly to a procedure developed by Spackman, More and Stein in 1958 [22]. The column eluent was mixed with ninhydrin reagent to react with the aminoacids. The colored compounds resulting from the reaction were analyzed at two different wavelengths, 440 and 570 nm. The quantitative analysis was carried out using Norleucine as an internal standard. The represented results correspond to a mean of three independent measurements.

2.3.2. Fourier transform infrared spectroscopy

To study and compare the chemical composition of both collagens, Fourier transform infrared spectroscopy (FTIR) under an attenuated total reflectance (ATR) (IRPrestige 21, Shimadzu) was carried out. Marine and bovine lyophilized collagen samples were mixed with potassium bromide (KBr) (1:100, wt%) and then uniaxially pressed to obtain transparent disks. Each infrared spectrum was the average of 32 scans collected at 2 cm⁻¹ resolution in the wavenumber region of 3500–500 cm⁻¹ at room temperature (RT).

2.3.3. Sodium dodecyl sulfate-polyacrylamide gel electrophoresis (SDS-PAGE)

The protein molecular mass analysis was studied by using a 7 % polyacrylamide SDS-PAGE characterization gel. SDS-PAGE was prepared by using reagents from sigma and casted on a Biorad Mini Protean II System. Solubilized collagen was mixed with a buffer and heated at 95 °C for 5 min into a digital thermoblock TD150P3 (FALC) until proteins denaturation. After, 8 µL sample loading volume (10 µg per lane) was used. Also, 3 µL of protein marker was loaded with the samples. Electrophoresis was carried out at 75 V for 15 min followed by 150 V until the frontline reached the lower part of the gel. After running, the gel was stained with Coomassie blue R-250 in methanol (50 %) and acetic acid (10 %) for 30 min followed by destaining with methanol (5 %) and acetic acid (7 %). Bovine type I collagen from Sigma was used as control.

2.4. Preparation of marine bioapatite particles extracted from blue shark teeth

The heads of mako shark *Isurus oxyrinchus* and blue shark *Prionace glauca* were boiled in water for 3 h for teeth removal. After, teeth were cleaned and washed, followed by drying at 60 °C for 24 h. For particle size homogeneity, the teeth were ground in a ball mill (Retsch MM2000) for 5 min, with an oscillation frequency between 90 and 100 Hz for powder size of 100 to 0.1 µm. The ground teeth were pyrolyzed at 950 °C for 12 h, to remove the organic material, with a heating ramp of 2 °C/min and a cooling ramp of 20 °C/min. The resulting particles of apatite were separated by sieves below 63 µm of particle size.

2.5. Apatite particles characterization

2.5.1. X-ray diffraction pattern

The crystallinity of the marine BAp particles was studied and compared with the synthetic origin Ap particles by using an x-ray diffractometer. The diffraction measurements were performed using a conventional Bragg–Brentano diffractometer (Bruker D8 Advance DaVinci, Germany) equipped with CuKα radiation. Data sets were collected in the 2θ range of 10–60° with a step size of 0.02° and 1 s for each step.

2.5.2. Coulter analysis

The physical characteristics (particle size and particles size distribution) of both the bioapatite (obtained from mako and blue shark teeth) and synthetic apatite powders were evaluated using a particle size analyzer (COULTER LS230, UK), with Fraunhofer optical model. This technique uses electrical impedance to measure the volume of particles as they individually pass through an aperture of defined size.

2.5.3. Scanning electron microscopy (SEM)

SEM analysis was used for two purposes: to study the morphology of the apatite powders and to study the produced scaffolds' surface properties. Dried samples were coated with gold to increase conductivity and were analyzed in a scanning electron microscope (JSM-6010 LV, JEOL, Japan) at 20 kV using different magnifications.

2.6. Scaffolding

2.6.1. Preparation of scaffolds

For scaffolds production, a freeze-drying technique was employed, as described before [18]. The isolated freeze-dried collagens were solubilized at 1.5 % (w/v) in 0.5 M acetic acid solution. After, marine BAP or synthetic hydroxyapatite (Plasma Biotall Ltd., UK) were added to the mColl and bColl solutions, respectively. The final mixtures had in their constitution 30 % of collagen and 70 % of apatite particles (w/w), resulting in 2 different scaffolds formulations: mColl:BAP and bColl:Ap. To increase scaffolds' stability, 1-ethyl-3-(3-dimethylaminopropyl)

carbodiimide (EDC) at 12.5 % (w/w) was added to promote collagen crosslinking. The reaction was carried at low temperatures (6 °C) for 4 h, being the mixture then poured into a mould and freeze-dried. To wash out any harmful residual compound, including unreacted crosslinking agent, all scaffolds were thoroughly rinsed with distilled water immediately before using in cell culture experiments. Scaffold matrices with cylindrical shape (6 × 5 mm) were used for structural characterization and *in vivo* assessment.

2.6.2. Characterization of scaffolds microarchitecture

The microstructure of the collagen-based composites scaffolds was analyzed using a high-resolution X-ray micro-computed tomography system (Skyscan 1272, Beuker, USA). Dried samples were scanned using a pixel size of 10 µm over a rotation step of 45° and rotation angle of 360°. Porosity, mean pore size, and interconnectivity were assessed after reconstruction of images stacks in a microCT-analyzer program by defining a threshold from 30 to 255, to distinguish the composite structure from the pore voids. To understand if the apatite particles were homogeneously distributed through the constructs, it was applied a threshold from 65 to 255.

2.6.3. Mechanical assays

The mechanical behavior of both marine and bovine collagen-based 3D constructs was assessed under compression mode using an INSTRON 5540 universal testing machine. Six replicates of each condition were tested with a crosshead speed of 2 mm/min and a load cell of 1 kN. The compressive modulus, a measure of material stiffness, was determined from the slope of the linear region at the beginning of the stress-strain curve.

2.7. In vivo evaluation of collagen-based composite scaffolds

2.7.1. Animals

Twelve male New Zealand White rabbits (age between 18 and 21 weeks) weighting 3.7–4.0 kg were supplied by a qualified laboratory animal supply center (La Granja cunícola San Bernardo, S.L., Tulebras, Navarra, Spain).

The animals were housed in individual enriched cages in the Animal Experimentation Service Facility of the University of Santiago de Compostela (Lugo, Spain) after the ethical approval (procedure code: 03/18/LU-002) as a randomized controlled trial with one inter-subject control.

Animals were maintained under conditions of temperature (15–21 °C), humidity, air renewal and cycle time (12 h alternating cycles of light and dark) controlled according to annex II of directive 86/609/EEC. After an acclimatization period of three weeks, animals were pre-medicated with Ketamine 25 mg/kg/i.m. (Ketamidol® 100 mg.mL⁻¹), medetomidine 50 µg/kg/i.m. (Sedorm® 1 mg.mL⁻¹) and buprenorphine 0.03 mg.kg⁻¹ (Bupaq® 0.3 mg.mL⁻¹). The anesthesia was maintained by inhalation of an O₂ and 2 % isoflurane mixture using a facemask.

2.7.2. Implants

Cylindrical shape (6 mm Ø X 5 mm height) collagen-based composites were tested. Two different materials and an empty control were randomly assigned to the left or right side according to a computer-generated randomization list until complete an *n* = 8. In total, 16 biomaterials and 8 empty defects were considered for 12 animals, being thus two conditions per animal. To avoid errors due to the implantation side, half of each biomaterial and half of the empty defects were associated to left femurs and half to rights. The trial period used was up to 12 weeks.

2.7.3. Surgical procedure

Bone defects with cylindrical shape (6 mm Ø X 5 mm height) were created under aseptic conditions in the distal lateral part of femoral condyle by using a trephine connected to a surgical motor (intrasurg

300, Kavo, Biberach, Germany) under irrigation. The defect was rinsed with sterile saline after the bone segment was removed and the biomaterial was implanted or the defect left empty, according to the plan. Then, the wounds were sutured using a 4–0 vicryl in deep planes and 3–0 nylon for the skin. The animals were monitored throughout the time, the pain was controlled in the first 5 days by using buprenorphine (0.01–0.03 mg/kg/i.m., Buprex, RB Pharmaceuticals) and meloxicam (0.2 mg/kg SC, Metacam, Boehringer). As a prophylactic antibiotic it was used enrofloxacin (Syvaquinol® 10 % oral) for 3 weeks. The animals were sacrificed with an intravenous overdose of sodium pentobarbital (Dolethal, Vétquinol) after sedation with Ketamine 25 mg/kg + medetomidine 50 µg/kg + buprenorphine 0.03 mg/kg. Subsequently, the distal femurs were recovered by dissection and the use of a bone saw. Specimens were immediately immersed in a 10 % buffered formalin solution for a minimum of 2 weeks until the time of processing. For identification, we use a code consisting of a number and a letter. The number indicated the animal (from 1 to 12) and the letter the side of the femur (right-R and left-L). All biomaterials were recovered.

2.7.4. Micro-CT of the defects filled with the biomaterials

To evaluate the *in vivo* regeneration of the bone defects created in the rabbit femoral condyles, all samples were micro-CT scanned using the Skyscan X-ray micro-computed tomography 1272 (Skyscan, Kontich, Belgium). Fixed samples were scanned with an aluminum/copper filter at 13 µm pixel size resolution with an X-ray source voltage of 90 kV and current source of 111 µA, 0.4 rotation steps and 2 averaging frames during 0 h:56 m:36 s of scanning. The micro-CT images were reconstructed with a NRecon program version 1.1.3 (Skyscan) and the reconstructed images were reoriented with a Dataviewer program version 1.17.0.0 (Skyscan) for subsequent analysis. To qualitatively assess the percentage of bone volume (new bone plus scaffold) it was applied a cylindrical region of interest (ROI) corresponding to the bone defect size filled with the different structures. Phantoms of 0.25 and 0.75 g.cm⁻³ were scanned and reconstructed with the same parameters for bone mineral density (BMD) calibration. A trained staff performed all analyses without knowing the material being analyzed.

2.7.5. Histomorphometry analysis

After micro-CT scanning, samples were subjected to the histology laboratory in Lugo (Veterinary faculty, USC, Lugo, Spain) to produce the thin ground sections in accordance with the method described by Donath [23]. Samples were introduced in individual sample holders, dehydrated in different graded ethanol series (70–100 %) and infiltrated with different graded mixtures of ethanol and glycometacrylate (Technovit 7200 VLC, Heraeus Kulzer, Werheim, Germany). Samples were maintained for almost three days in each concentration, with continuous agitation, then were polymerized and heated at 37 °C for 24 h to ensure a complete polymerization. Each block containing a rabbit femoral condyle was prepared and several sections were obtained until obtaining circular sections with the defect. Sections were polished using a grinding machine (Exakt Aparatbau, Hamburg, Germany) using 1200 to 4000 grit silicon carbide papers (Struers, Copenhagen, Denmark) until samples had a thickness of about 40 µm. The slides were then stained using the Levai–Laczkó method [24].

After histology preparation, the images were captured using an optical microscope (BX51, Olympus, Tokyo, Japan) connected to a digital color camera (DP71, Olympus, Tokyo, Japan) and which has a motorized plate (Märzhäuser, Steindorf, Germany). The obtained images were aligned and connected automatically obtaining complete images of the bone and the implanted biomaterial at a magnification of 40×. To quantify bone-like tissue, a circular ROI with the same diameter of the defect was drawn. With Adobe Photoshop a blind examiner painted the new bone formed inside this ROI and the % of new bone in this area was measured in Cell Sens dimension software (Olympus, Tokyo, Japan).

3. Results and discussion

3.1. Protein profile

Collagen has been extracted from different animals, with three main methods being reported, resulting in salt-soluble collagen (SSC), acid-soluble collagen (ASC), and pepsin-soluble collagen (PSC) [25]. The properties of the produced biopolymer are directly affected by the species of origin and by the selected method for its extraction, with marine-origin collagens arising recently as alternative to the well-established mammal collagens for biomedical application [25]. Aiming to better assess the potential of blue shark collagen for regenerative medicine, this was compared with bovine collagen, gold standard material in biomedical applications, with both being extracted with an acid-based method, to finally prepare collagen-based composites for TE (Fig. 1 A). The wide range of amino acids, typically characteristic of collagen protein, was demonstrated by quantitative analysis of the amino acid profile (Fig. 1 B). The extracted collagens had a similar profile, being rich in glycine (Gly), proline (Pro) and hydroxyproline (OHPro). Glycine was the highest prevalent amino acid in both collagens, representing around 30 % of the total protein. This finding is in a good agreement with other studies, since glycine appears regularly at every third residue throughout the collagen molecules, particularly within the triple helix [26,27]. Pro (11.2 % of bovine collagen and 10.1 % of marine collagen) and OHPro (8.2 % and 6.5 % of bovine collagen and marine collagen, respectively) were found within the range already describe in the literature [22,28]. Blue shark collagen had a lower Pro and OHPro content in comparison with bovine collagen, following the same tendency globally observed between collagens from marine organisms and from mammals. Animal species living in aquatic environment have lower body temperatures comparatively to terrestrial mammals because of their evolutionary adaptation (in general, marine environment is colder than terrestrial ecosystems and the marine organisms lack the physiological mechanism to maintain a certain body temperature) and the contents of these amino acids are known to be related with the thermal stability of collagens. In fact, these amino acids hold a critical role in the maintenance of the triple-helix structure integrity, which have high influence on collagen denaturation temperature [29].

FTIR was performed to chemically characterize the extracted collagens (Fig. 1 C). The spectra showed very similar profiles for both tested collagens, with the presence of the characteristic peaks of amide A, amide B, amide I, amide II and amide III, assigned to the collagen protein. Amide A peak, typically observed between 3000 and 3500 cm⁻¹, was seen at 3320 cm⁻¹, as a result of the N–H stretching vibration associated with the intermolecular hydrogen bonding in the carboxyl groups. The amide B peak, relative to the asymmetric and symmetric stretch of CH₂, was identified at 2918 cm⁻¹, even though being less evidenced for *Prionace glauca* collagen. Strong peaks around 1660 cm⁻¹ and 1543 cm⁻¹ associated with C=O stretch (amide I) and N–H deformation (amide II), characteristics of proteins, were found in spectra of both collagens. The C–N stretch of amide III was located at 1243 cm⁻¹. The results are in accordance with the chemical pattern of collagen [26].

Shark and bovine skin collagen, isolated in this work, were identified as being mainly type I collagen given the characteristic electrophoretic profile obtained with SDS-PAGE (Fig. 1 D). The characteristic alpha 1, alpha 2 and beta components, with alpha 1 being more intense than alpha 2, typically attributed to type I collagen in mammals, were found in both extracted collagens. This finding matches well with the available bovine type I collagen commercialized by Sigma and used as reference material, which suggests the suitability of using blue shark *Prionace glauca* skins as a promising alternative source of collagen.

3.2. Apatite and bioapatite particles characterization

Calcium phosphate-based materials are often employed to stimulate

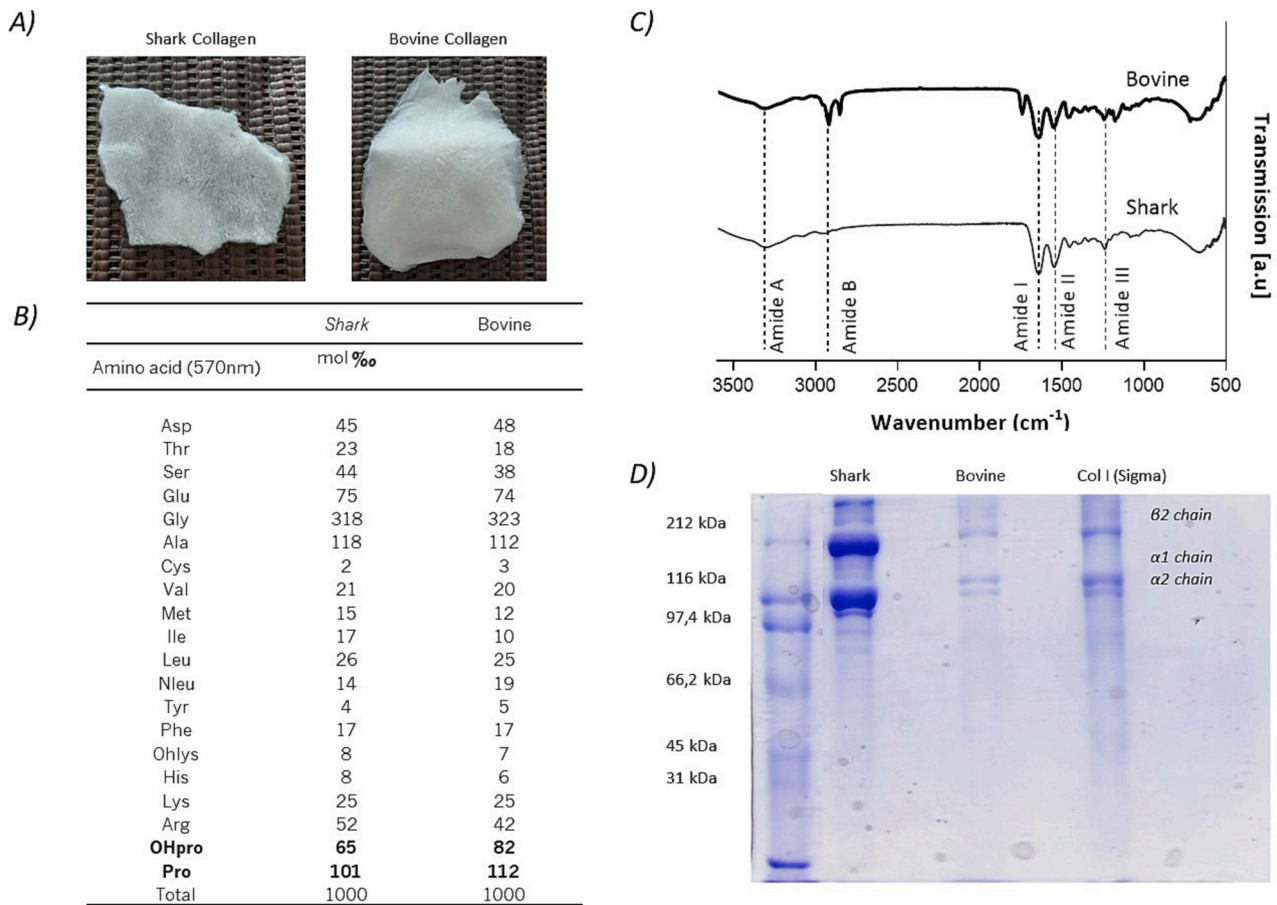


Fig. 1. – Characterization of blue shark and bovine collagen. A) Lyophilized shark and bovine collagen; B) Amino acid composition. C) FTIR spectra, showing the characteristic profile of collagen protein, namely the several amide peaks. D) SDS-PAGE of shark and bovine extracted collagen exhibiting representative band pattern ($\alpha 1$, $\alpha 2$ and β), together with reference type I collagen (commercial sample). (For interpretation of the references to color in this figure legend, the reader is referred to the web version of this article.)

bone formation, which is affected by ceramic crystallinity, crystalline phase, calcium/phosphorus ratio, topography and surface charge. Consequently, this process enables the release of essential calcium and phosphate ions crucial for bone mineralization [30,31]. Chemically synthesized apatite particles, like hydroxyapatite (HAp, $\text{Ca}_{10}(\text{PO}_4)_6(\text{OH})_2$), are mainly obtained from the reaction of calcium with phosphate solutions under particular pH and temperature conditions. Despite being the first choice within all calcium phosphates sources when considering biomedical use, the distinctive physico-chemical properties of synthetic HAp when compared with natural hydroxyapatite ends in a lower biological activity [32,33]. It has been hypothesised that extracting hydroxyapatite from natural sources, like bones and teeth, result in apatite particles with preserved chemical and structural properties, which leads to the exploration of new possible sources. In the present work, the potential of using teeth from *Isurus oxyrinchus* and *Prionace glauca* sharks to obtain a biological apatite material was further explored [17,18]. The thermal conversion of shark teeth, considered a biowaste by the fishing industry, resulted in samples exhibiting an x-ray diffraction pattern characteristic of a crystalline material. The XRD patterns of marine bioapatite particles presented in Fig. 2 A confirmed the presence of two phases (one apatite and other non-apatite) with sharp and well defined diffraction peaks, confirming that the pyrolysis was efficient, with no trace of organic material after the heat treatment [18]. The apatite- CaF ($\text{Ca}_5(\text{PO}_4)_3\text{F}$) phase (ICDD 04-016-2909) presented the most intense peaks at 31.87 and 33.04 for the crystal planes (2 1 1) and (300), while the non-apatite phase, whitlockite (ICDD 04-079-2186), had the most intense peaks at 31.24 and 34.59 for

the crystal planes (0 2 10) and (2 2 0) (Fig. 2 A). According to our previous work [18], the marine bioapatite particles extracted from teeth of shark have in their composition, in addition to calcium and phosphorus, other ions such as fluor, magnesium, sodium, among others, leading to lower Ca/P ratio, justifying the formation of non-apatite phase (whitlockite) [34]. Additionally, the presence of Mg^{2+} promotes the decomposition of apatite phase into whitlockite, because the ionic radius of Mg^{2+} is smaller than that of Ca^{2+} [35]. Commercial synthetic apatite exhibited the characteristic pattern of hydroxyapatite (ICDD 01-089-4405), as expectable, without any other phase.

Particle/agglomerate size distributions (PSD) of marine BAp and commercial Ap powders are presented in Fig. 2 B. As depicted in the graph, PSD of Ap resulted in a sharper peak when compared with BAp, suggesting a higher homogeneity of particle size of the former. The measured average particle/agglomerate sizes were 3.511 μm for Ap particles and 17.95 μm for BAp particles (>5 times higher), even though, for the BAp the particle size ranged from 1 to 60 μm . SEM micrographs (Fig. 2 C) shows the morphological features of BAp and Ap powders. Both powders consisted of small agglomerates with distinctive shaped particles: the BAp particles showing mostly roundish forms, while the Ap had rod-like particles. Comparing the results obtained by coulter analysis with SEM micrographs, it is shown that individual particles of BAp are actually smaller than initially considered, and the high degree of particles agglomeration could be responsible for the higher values of mean particle size obtained from coulter analysis.

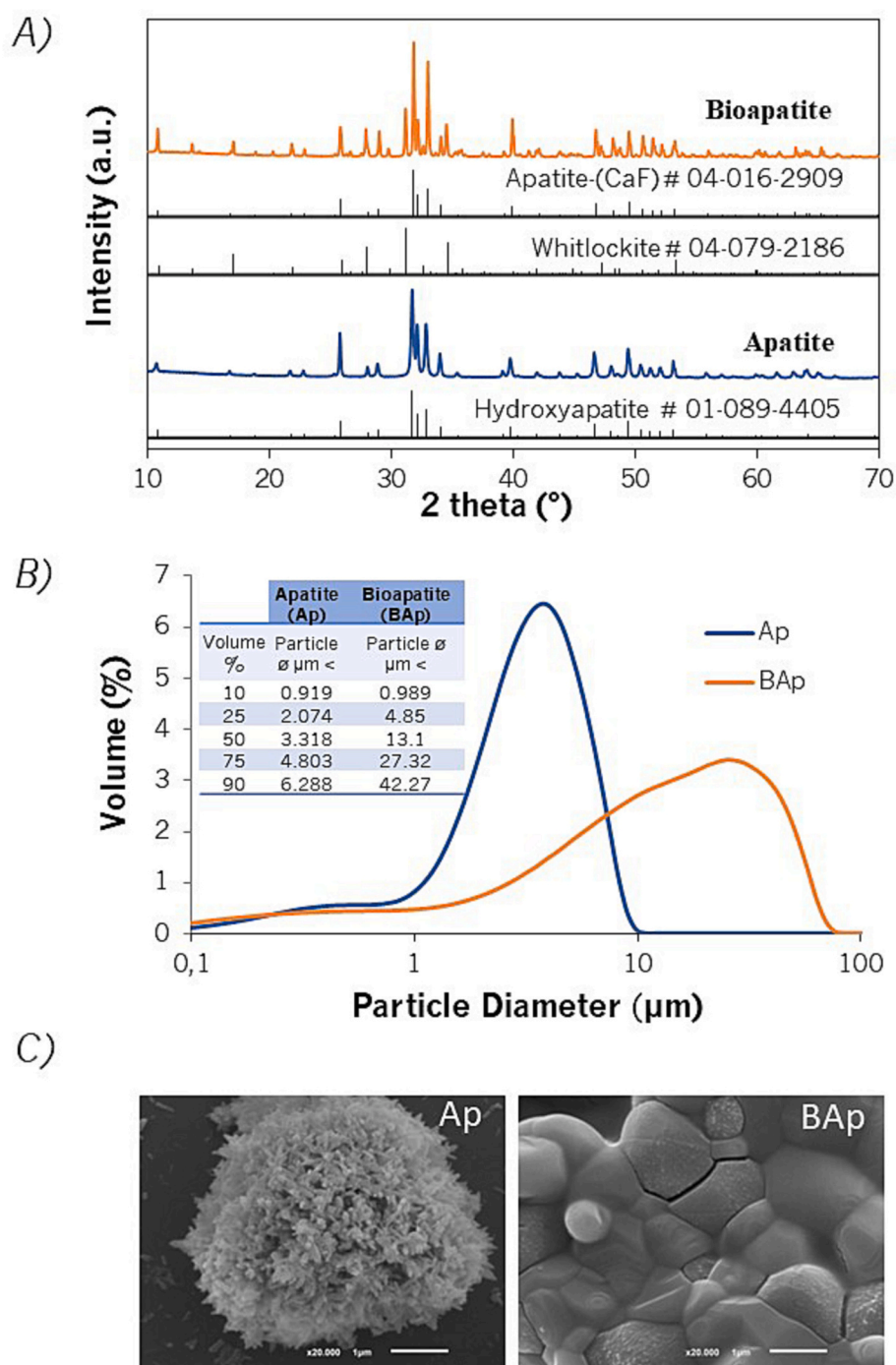


Fig. 2. – Synthetic Apatite (Ap) and shark teeth-derived Bioapatite (BAP) particles characterization. A) X-ray diffraction pattern. B) Coulter analysis illustrating particle size and distribution. C) SEM morphological analysis.

3.3. Microstructure of scaffolds

For the 3D porous structures fabrication, a conventional freeze-drying process was applied. In comparison with other conventional processing methodologies of scaffolds production, like gas foaming and salt leaching, freeze-drying is still considered the most useful technique for fabrication of porous structures with natural polymers [36–38]. It is an advantageous technique for collagen-based scaffolding production because it can almost preserve the native structural form and the biological properties of collagen [39]. The ice crystals growth during the freezing process allows the formation of porous structures and, at same time, the elimination of the solvents during the lyophilization process,

without resulting in polymer degradation [36]. SEM microscopy was employed to determine scaffolds' surface morphology. As depicted in Fig. 3 A, both collagen-based scaffolds revealed a regular distribution of pores with slightly macroscopic differences. It seems that mColl:BAP scaffold formulation resulted in larger pores in comparison with the bovine-based formulation. In contrast, it looks that there was an higher tendency for particles agglomeration (see highly magnified SEM images) in the bColl:Ap condition.

Scaffolds microarchitecture features, namely porosity, pore size and interconnectivity, have been described to develop a crucial role for fate of seeded cells, by promoting nutrients and oxygen diffusion into the interior of the structures [40]. Such parameters cannot be rigorously

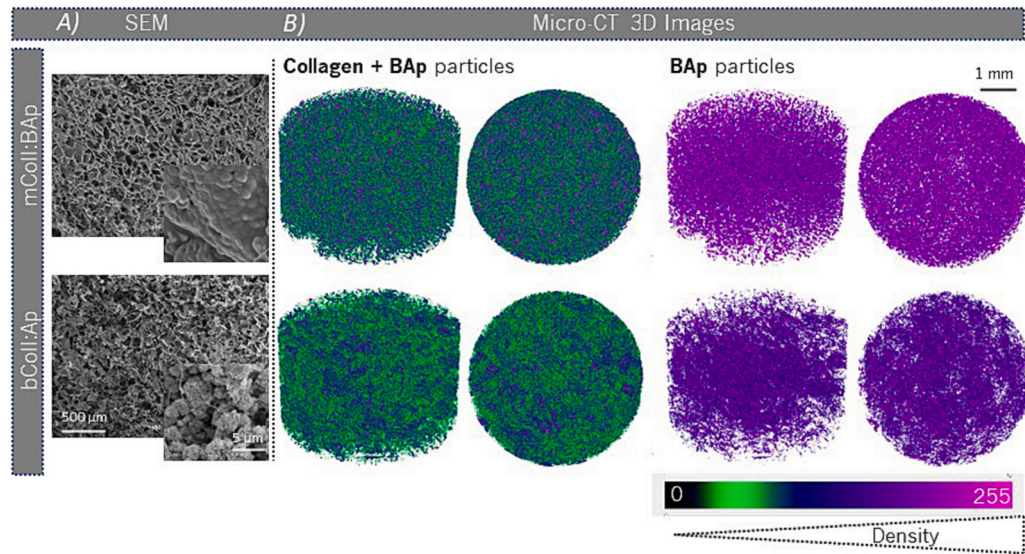


Fig. 3. – Microarchitecture characterization of the produced composite scaffolds. A) Morphological characterization of scaffolds by SEM analysis. B) Qualitative micro-CT images with green representing less dense material (collagen) and in purple the Ap and BAP particles. (For interpretation of the references to color in this figure legend, the reader is referred to the web version of this article.)

controlled by freeze-drying technique, but can be modulated by varying materials concentration, crosslinking degree and freezing temperature and time. To assess scaffolds internal microarchitecture, quantitative and qualitative micro-CT analysis was performed. To differentiate organic and inorganic components on the sample, a color coding was employed according to materials density, from 0 to 255 (density scale).

The green color refers to collagen, while purple represents the densest material, which corresponds to the Ap or BAP particles. The qualitative results (Fig. 3 B) showed a better distribution of BAP throughout the marine collagen when compared with Ap distribution within bovine collagen. This is represented by the higher homogeneity of the purple color in the marine-based composite scaffolds, suggesting the feasibility

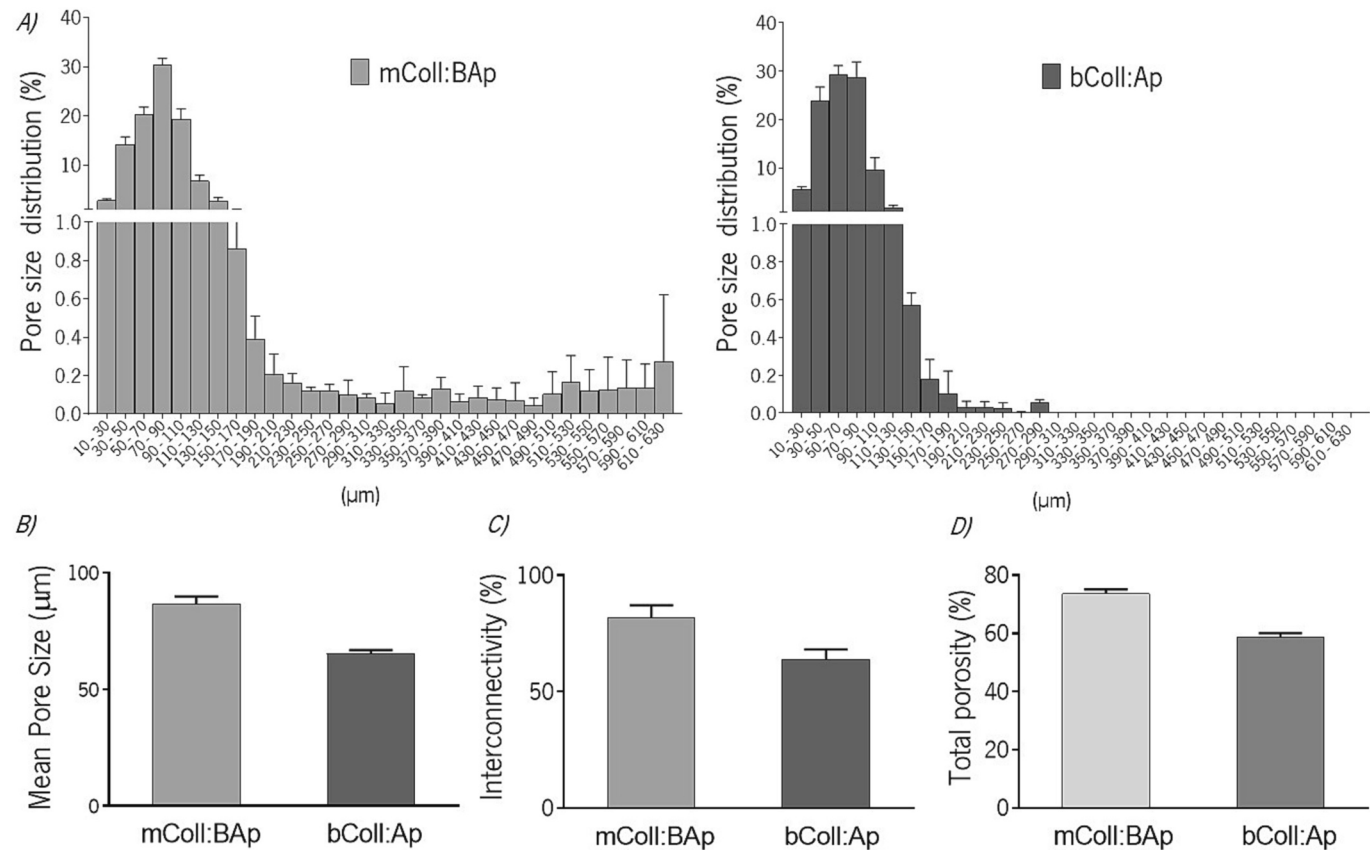


Fig. 4. – Quantitative micro-CT analysis of the produced collagen-based composite scaffolds. A) Pore size distribution. B) Mean pore size (µm), C) Interconnectivity (%) and D) Total porosity (%). Mann Whitney test was used to compare the two conditions, with a p value lower than 0.05 ($*p < 0.05$) considered statistically significant. No statistical differences were observed between groups.

of the method used for the production of these scaffolds.

Quantitative results of micro-CT for the mean pore size of the scaffolds was calculated in a CT analyzer program after selection of a threshold from 30 to 255 (to discard void spaces) and showed higher values for the mColl:BAP ($86.8 \pm 3.1 \mu\text{m}$) when compared with bColl:Ap ($65.3 \pm 1.5 \mu\text{m}$) formulation (Fig. 4B). Thus, it is expected that the cells will colonize faster and efficiently the marine based composite scaffolds. Moreover, it is important to mention that both groups of scaffolds showed a porous architecture with a pore size distribution from 10 to 600 μm , with >50 % of pores ranging from 70 to 150 μm (Fig. 4A). These values fall within the required range to yield positive outcomes in the context of their application to bone tissues, as previously demonstrated [15,41,42]. Accordingly, to the literature pores with different sizes fulfill distinctive roles. Pores with lower sizes (<100 μm) are required to allow an enhanced permeability to tissue fluid, generating additional sites for cell adsorption [43]; contributes to the transformation of primary macrophages into the M2 type, leading to an upregulation of anti-inflammatory gene expression, which suppresses the host immune response to grafts [44]; and have been found to promote cell adhesion due to their large surface area. Larger pores (>100 μm) promote cell infiltration and colonization while facilitating the process of angiogenesis [45]. [46]. In an attempt to explore the potential of using hydroxyapatite particles obtained from fish bones of salmon, Lowe et al. prepared 3D composites scaffolds by freeze-drying technique, which exhibited pore size ranging from 23 to 354 μm that revealed to be adequate features to induce periosteum-derived mesenchymal stem cells proliferation and mineralization [47].

In addition, the processing methodology used for scaffolds production resulted in pore interconnectivity (Fig. 4C) varying between $81.9 \pm 4.5 \%$ and $63.8 \pm 4.36 \%$ for mColl:BAP and bColl:Ap, respectively, although no significant statistical differences were observed. High interconnective porous structures are greatly desired for nutrients perfusion and oxygen transport throughout the entire structure, which ultimately sustain their positive biological performance. Currently, it is widely accepted that scaffolds should feature a well-distributed and interconnected network of pores to provide osteoinductive properties.

The lowest porosity ($58.6 \pm 1.5 \%$) was found for the bColl:Ap formulation comparatively to mColl:BAP ($73.6 \pm 1.5 \%$) (Fig. 4D). It is believed that the higher agglomeration of Ap within the bovine collagen matrix, as aforementioned, reduced the nucleation spots for ice crystals formation and growth, resulting in less porous scaffolds.

4. Mechanical properties

Bioengineered scaffolds should provide mechanical structural support and biological cues for cell attachment, while new tissue is formed. Internal scaffolds' microarchitecture, including porosity, pore size and interconnectivity are important features to determine the final

mechanical properties. Despite the adequate biochemical features and promised biocompatibility, engineered collagen scaffolds are normally characterized by limited mechanical strength [48]. A popular approach to enhance the collagen mechanical strength is its combination with other robust components, such as ceramics, as it was adopted in this work. The mechanical properties of the developed composite scaffolds were assessed under uniaxial compression load. The bioapatite reinforced shark collagen scaffolds displayed a higher compression modulus when compared with apatite strengthened bovine collagen scaffolds (Fig. 5). The obtained results can be associated with the higher viscosity of marine collagen due to the selected conditions of processing. The temperature chosen for the crosslinking reaction (4 °C) was advantageous to increase fish collagen viscosity. However, the same was not observed for bovine collagen that is less viscous at lower temperatures. The motivation to select this temperature was based on previous works that reported that marine collagens have inferior viscosity properties and denatures at high temperatures, including blue shark collagen [29]. The small differences in terms of biochemical composition can affect collagen behavior, as collagen triple helix structure is highly influenced by the amino acid composition. The lower content of glycine, Pro and OHPro of marine collagen demands a strict control of temperature. In addition, it is described in literature that, generally, unmodified fish origin collagens present lower mechanical strength than the ones extracted from bovine sources, since it is less crosslinked [49]. However, the mechanical properties can be modulated by altering collagen concentration and by applying physical or chemical crosslinking agents. The mechanical properties of the scaffolds herein presented indicate that the chemical reaction with EDC combined with freeze-drying resulted in scaffolds with different properties, being advantageous in improving the mechanical behavior of the blue shark collagen:bioapatite scaffolds comparatively to the bovine collagen:synthetic apatite ones. This result can also be strongly related with the physicochemical properties of fluoride-enriched hydroxyapatite. Previous studies demonstrated that fluoride-enriched apatites increased the mechanical strength of hydroxyapatite [50]. Finally, both type of scaffolds presented a spongy-like behavior with stress-strain curves characteristic of highly ductile materials. This feature is of great interest to pursue the regeneration of several tissues, including bone defects, due to its easy surgical handling and proper fixation to the site of implantation.

4.1. *In vivo* assessment – Defects regeneration capabilities

Aiming to evaluate the *in vivo* potential of the collagen:apatite produced scaffolds, bone defects were created in the lateral femoral condyles of New Zealand rabbit models. The materials were implanted in both knees, right and left, with a random distribution. An empty group was used as the control of the experiment. The experimental animals recovered well from the surgical procedure and remained in good health

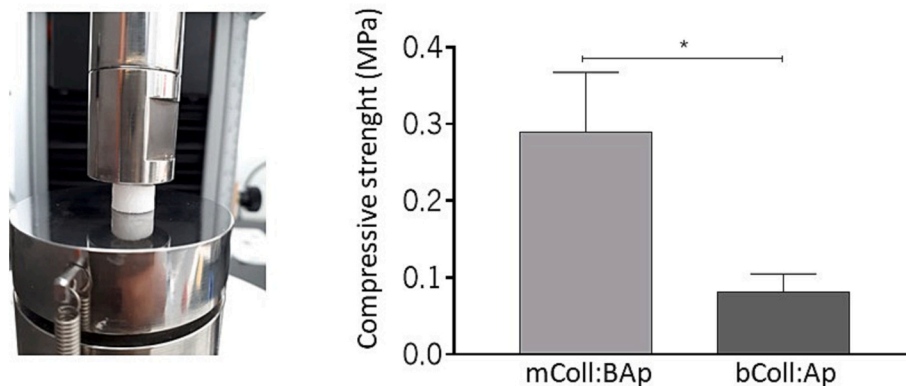


Fig. 5. – Mechanical properties of collagen-based composite scaffolds assessed by uniaxial compression tests. Mann Whitney test was used to compare conditions, with a p value lower than 0.05 considered statistically significant (* $p < 0.05$).

afterward. Only three of them showed weight loss at termination which was related to osteoarthritis signs induced by a chronic patellar luxation described in the necropsy. This complication is frequent in this model and did affect one control and one mColl:BAP knees. To evaluate the bone defects regeneration, micro-CT analysis and histomorphometry of femoral condyles were performed 12 weeks post-implantation. Fig. 6 represents overall the process from the materials origin to materials implantation and analysis.

Histologically both materials showed high resorption rates, although the mColl:BAP group showed the presence of residual material at 12 weeks post-implantation. If showed, a discrete presence of multinucleated macrophage-like cells was detected around the particles, but without the presence of other inflammatory cells like neutrophils or lymphocytes. Some graft particles were embedded in the newly formed bone matrix. New lamellar bone formed was similar to pristine bone, with a structure typical of the cancellous bone.

The findings suggested bone-like tissue formation in the defects implanted with both constructs (Fig. 7 A,B and Fig. 8 A,B). Twelve weeks after implantation, the percentage of mineralized tissue calculated in a micro-CT analyzer program after a ROI selection were 17.9 ± 6.9 % for mColl:BAP and 12.9 ± 7.6 % for bColl:Ap, respectively, without significant statistical differences comparing with empty defects (9.6 ± 6.3 %) (Fig. 8 C). Despite the similar chemical composition of both polymeric-ceramic materials, and although no statistical differences were observed between them, the results suggested an higher tendency for mineralized tissue formation in the mColl:mBAP implanted defects. The defects filled with the marine collagen-apatite composites did show

comparable with other ceramic-based materials that demonstrated around 20 % of new bone formation [51–53]. Moreover, it could be observed that the mColl:mBAP structures were not completely degraded and the bone-like tissue has grown into the middle of the implanted mColl:BAP material (highlighted by yellow arrows in Fig. 7 A,B and Fig. 8 A,B). This result could be greatly influenced by the good pores interconnectivity of the implanted structure that allows body fluid circulation, vascularization and cell migration promoting new tissue formation [54]. Vascularization and appropriate angiogenic properties are crucial features to determine the success of bioengineered scaffolds for bone since bone is a high vascularized tissue. A minimal pore size of 100 μm has been reported to allow bone tissue formation inside the pores of composites, being pores with diameters ranging from 200 to 400 μm considered optimal [55].

For bColl:Ap implanted condyles, in general, there was no residual material inside of the created defects. Such results are potentially associated to the calcium-phosphates and scaffolds properties. The resorption or degradation rate of a material and bone formation is highly dependent on the physicochemical composition of the ceramic part. The biodegradation of calcium phosphates-based systems increases as the crystal and grain size decreases. In addition, materials with low mechanical properties are faster degraded [56]. Bovine collagen-apatite structures degrade faster perhaps due to the finer crystal grains of the apatite particles and the poor mechanical properties of these constructs when compared with the mColl:BAP composites. Particles with bigger sizes and structures with improved cohesiveness and mechanical properties, like the mColl:BAP implanted materials, result in slower

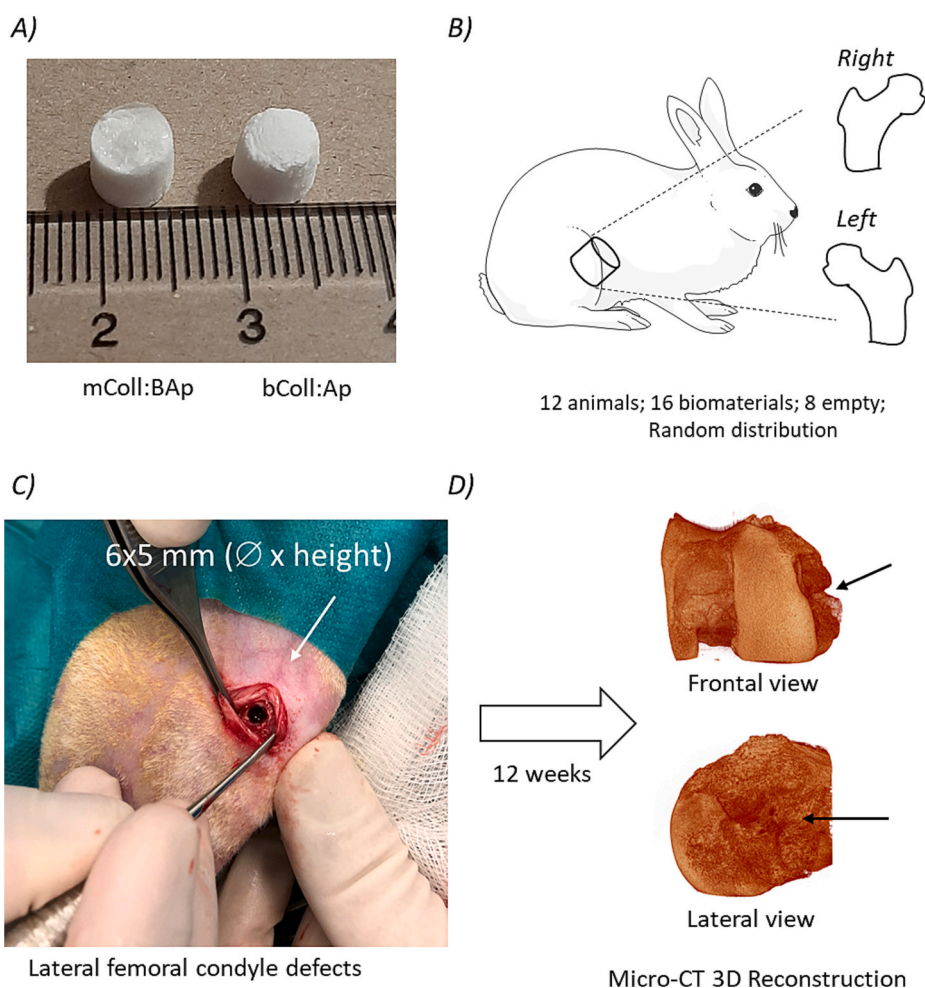


Fig. 6. – A) Collagen-based composite scaffolds, bColl:Ap and mColl:BAP. B) Schematic representation of the experimental design for materials implantation. C) Surgical procedure. D) Micro-CT evaluation of the regenerated defects.

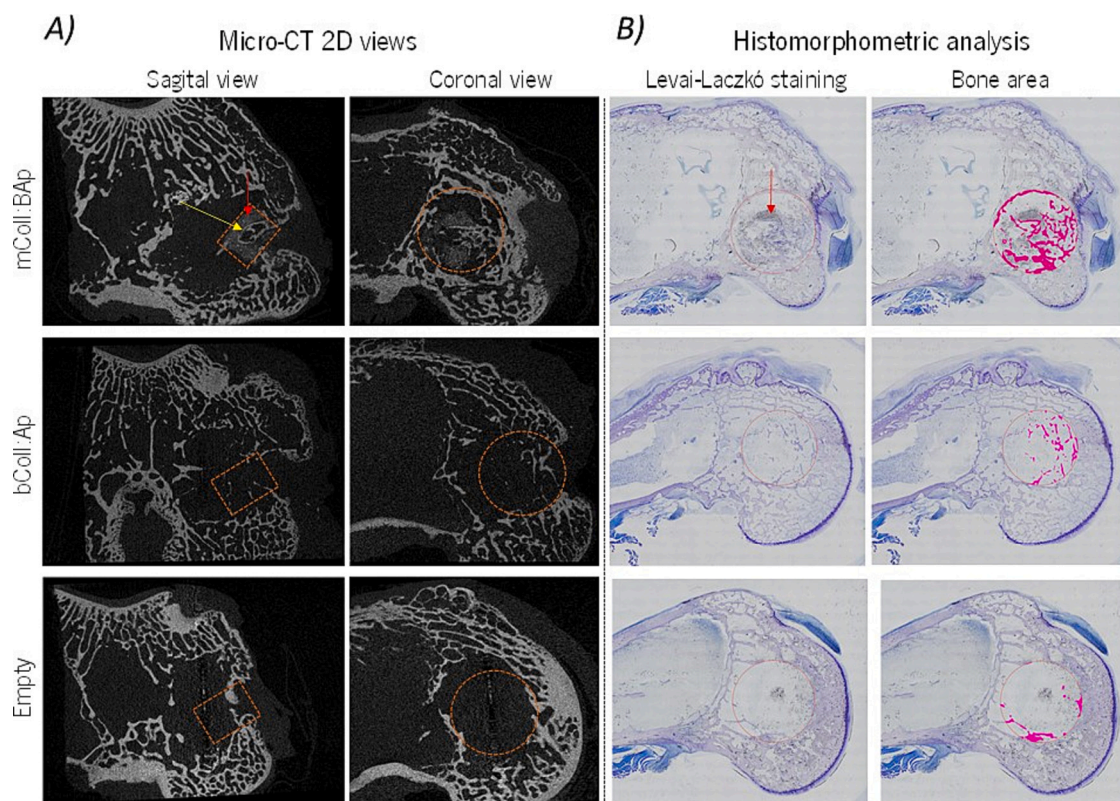


Fig. 7. – Micro-CT qualitative assessment of the regeneration of bone defects in rabbit femoral condyles treated with mColl:BAP or bColl:Ap composite scaffolds (empty defect used as control) 12 weeks after implantation. A) 2D micro-CT images from a sagittal and coronal view. Lesioned areas (Region of interest (ROI)) of femoral condyle were highlighted in orange. B) Histomorphometric analysis of the regenerated condyles. Leval-Laczko staining showed the formation of new bone at pink color. (For interpretation of the references to color in this figure legend, the reader is referred to the web version of this article.)

degradation rates, as could be observed in Fig. 7 A,B and Fig. 8 A,B. In addition, fluoride-enriched apatite (that is present in the marine bioapatite) has been described as an effective way to decrease the apatite solubility, which might have also contributed to slow down the degradation rate of the mColl:BAP construct [57].

The outcomes obtained from the histomorphometric analysis related to the newly formed bone-like tissue are well correlated with the micro-CT results. After 12 weeks, the defects implanted with mColl:BAP constructs were occupied with 13.1 ± 7.9 % of mineralized tissue. Similar amounts of bone-like tissue, 10.4 ± 3.2 %, were also found for bColl:Ap, and smaller amounts, 6.8 ± 4.3 %, for the empty condition (Fig. 8 D). The two methods of analysis, micro-CT and histomorphometry, were complementary with the respective results showing the same tendency, although small differences in terms of percentage could be observed, which may be attributed to the fact that the histological analyses were performed only in 2D slides, representative of the central zones of the defects, while the micro-CT analyses explored the 3D volume of the defect zone.

Also, in other studies, small differences were observed when comparing the histological to the micro-CT assessments [58], which were attributed to the difficulty to discriminate by radiographies (micro-CT) the implanted material from the new formed bone due to the similarity in terms of density and mineral contents. This may provide a further explanation for the higher amount of bone found with micro-CT in comparison with the histological analyses (only stains bone) that easily separates residual materials and newly formed bone.

The similarities obtained between both collagen-based composites support the use of marine-origin materials as a viable and promising strategy for bone TE scaffolding. The lack of significant statistical differences between the implanted materials with the empty group can be associated with the type of tissue that was formed. The fact of having a

similar percentage of bone volume does not mean that tissues with the same quality were produced in the three assessed groups. Studies have been reporting the incidence of fibrous tissue formation in the absence of bioengineered constructs, since the lack of bioactive cues does not attract the migration of the desired cells into the defect, while promoting the migration of fibroblasts and blood vessels that fill the empty areas with fibrous tissue [59]. In addition, the preserved mColl:BAP construct 12 weeks post-implantation can be advantageous to provide an adequate long-term mechanical support. It is well-known that a balance between the degradation rate of the structures and the new bone formation is a key factor to determine the success of the implanted materials to regenerate the target tissue [51]. In contrast, the fast degradation rate of the bovine-based structures can compromise an adequate long-term mechanical support.

In terms of trabecular separation (Fig. 8 E), that corresponds to the void spaces (pores) amid the trabeculae, it could be observed smaller pores for the mColl:BAP when compared with bColl:Ap. Probably, in the former case the remaining material together with the newly formed tissue left room for a well-organized matrix distribution, which better guided the tissue regeneration. The trabecular bone thickness (Fig. 8 F) did not show significant differences between both types of composite scaffolds and with the empty group. Bone mineral density calculated from calibrated phantoms revealed similar results, 0.32 ± 0.10 g.cm⁻³ for mColl:BAP and 0.37 ± 0.13 g.cm⁻³ for bColl:Ap composite scaffolds (Fig. 8 G), which are within the range described in the literature for rabbit models bone density [53,60].

Taken together, the results of the physicochemical characterization of collagen-based composite scaffolds and their performance on *in vivo* regeneration of bone tissue in rabbit model suggest the use of marine origin biomaterials as an effective and sustainable alternative to mammals-derived or synthetic materials for the engineering of bone

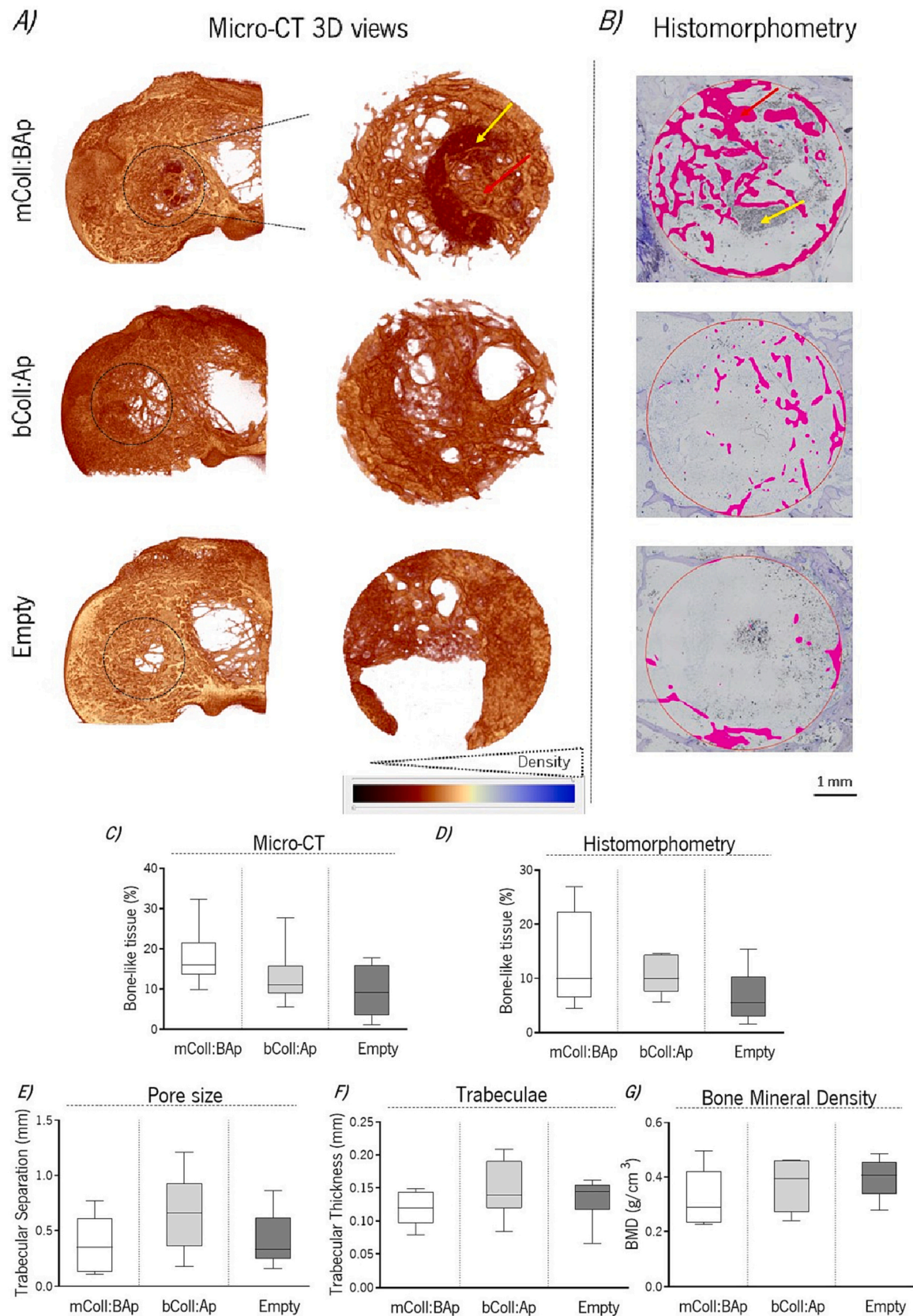


Fig. 8. A) 3D reconstruction of rabbit femoral condyles and the volume of interest (VOI) used for the quantitative analysis, defined as a cylindrical shape of 5×6 mm ($\varnothing \times$ height), which coincides with the projected defect filled with the different scaffolds. B) Histomorphometric analysis of new tissue formation in the selected ROIs. C) Percentage of bone-like tissue by micro-CT. D) Percentage of bone-like tissue by histomorphometry. E) Trabecular separation (mm). F) Trabecular thickness (mm). G) Bone mineral density (g/cm^3). Results are the median (line) \pm standard error of 8 samples per structure condition. Statistical analysis was performed using Kruskal-Wallis test with Dunn's Multiple comparison Test ($*p < 0.05$). There were no significant differences between groups.

tissue in a regenerative medicine context.

5. Conclusions

Composite scaffolds were produced by freeze-drying from formulations combining collagen and bioapatite derived from shark skin and teeth, respectively, and bovine collagen and synthetic hydroxyapatite, considered gold standard in biomedical research, with both types of scaffolds showing similar morphology but the marine-derived composites exhibiting higher compression modulus.

Qualitative and quantitative micro-CT and histomorphometry results of femoral condyles anatomy 12 weeks post-materials implantation showed regeneration capabilities for both – bovine and marine-based - implanted formulations. Tissue quantified inside the defect did not significantly vary between groups treated with each of the scaffolds' formulations. However, the marine-based composites demonstrated a higher tendency for bone-like tissue formation, around 17 and 13 %, quantified by micro-CT and histomorphometry, respectively.

The results suggest that the combination of blue shark collagen and bioapatite particles could result in 3D composites structures with bone regeneration capabilities, being an attractive choice to regenerate bone defects.

CRediT authorship contribution statement

Gabriela S. Diogo: Conceptualization, Formal analysis, Investigation, Methodology, Writing – original draft, Writing – review & editing. **Maria Permy:** Formal analysis, Investigation, Methodology. **Catarina F. Marques:** Formal analysis, Investigation. **Cármén G. Sotelo:** Resources. **Ricardo I. Pérez-Martín:** Resources. **Julia Serra:** Investigation, Resources. **Pio González:** Formal analysis, Resources. **Fernando Munõz:** Formal analysis, Investigation, Methodology. **Rogério P. Pir-raco:** Writing – review & editing. **Rui L. Reis:** Funding acquisition, Supervision, Validation. **Tiago H. Silva:** Funding acquisition, Supervision, Validation, Writing – review & editing.

Declaration of competing interest

The authors declare that they have no known competing financial interests or personal relationships that could have appeared to influence the work reported in this paper.

Data availability

No data was used for the research described in the article.

Acknowledgments

This study was funded by the Portuguese Foundation for Science and Technology (FCT) under the scope of the BiogenInk project (M-ERA-NET2/0022/2016), by European Regional Development Fund through INTERREG Spain-Portugal Programme, under the scope of 0245.IBER-OS_1_E project, through INTERREG Atlantic Area Programme, under the scope of BLUEHUMAN (EAPA_151/2016) project and through Northern Portugal Regional Operational Program (NORTE 2020), under the scope of Structured project NORTE-01-0145-FEDER-000021. The Doctoral Programme NORTE-08-5369-FSE-000044 supported by NORTE 2020, under the PORTUGAL 2020 Partnership Agreement, through the European Social Fund, is also greatly acknowledged by the PhD fellowship of GSD. RP and CM thank FCT for the research contracts IF/00347/2015 and CEECIND/04687/2017, respectively. The authors are also thankful to the Centro Tecnológico del Mar (CETMAR, Vigo, Spain) and COPEMAR SA (fishing company, Spain) for the kind offer of the fish by-products used for the production of collagen.

References

- [1] T.T. Roberts, A.J. Rosenbaum, Bone grafts, bone substitutes and orthobiologics: the bridge between basic science and clinical advancements in fracture healing, *Organogenesis* 8 (4) (2012) 114–124.
- [2] E. García-Gareta, M.J. Coathup, G.W. Blunn, Osteoinduction of bone grafting materials for bone repair and regeneration, *Bone* 81 (2015) 112–121.
- [3] E.T. Moghadam, et al., Current natural bioactive materials in bone and tooth regeneration in dentistry: a comprehensive overview, *J. Mater. Res. Technol.* 13 (2021) 2078–2114.
- [4] S. Caddeo, M. Boffito, S. Sartori, Tissue engineering approaches in the design of healthy and pathological in vitro tissue models, *Front. Bioeng. Biotechnol.* 5 (2017) 40.
- [5] A. Sionkowska, et al., The review of versatile application of collagen, *Polym. Adv. Technol.* 28 (1) (2017) 4–9.
- [6] T.H. Silva, et al., Marine origin collagens and its potential applications, *Mar. Drugs* 12 (12) (2014) 5881–5901.
- [7] N. Nagai, et al., In vitro growth and differentiated activities of human periodontal ligament fibroblasts cultured on salmon collagen gel, *J. Biomed. Mater. Res. A* 82 (2) (2007) 395–402.
- [8] J. Elango, et al., Rheological, biocompatibility and osteogenesis assessment of fish collagen scaffold for bone tissue engineering, *Int. J. Biol. Macromol.* 91 (2016) 51–59.
- [9] H.-H. Hsu, et al., Chondrogenic differentiation of human mesenchymal stem cells on fish scale collagen, *J. Biosci. Bioeng.* 122 (2) (2016) 219–225.
- [10] M.T.I. Mredha, et al., Anisotropic tough double network hydrogel from fish collagen and its spontaneous in vivo bonding to bone, *Biomaterials* 132 (2017) 85–95.
- [11] H. Mori, et al., Development of a salmon-derived crosslinked atelocollagen sponge disc containing osteogenic protein-1 for articular cartilage regeneration: in vivo evaluations with rabbits, *BMC Musculoskelet. Disord.* 14 (1) (2013) 174.
- [12] J. Hadzik, et al., A silver carp skin derived collagen in bone defect treatment—a histological study in a rat model, *Ann. Anat./Anat. Anz.* 208 (2016) 123–128.
- [13] A.M. Hassanbhai, et al., In vivo immune responses of cross-linked electrospon-tilapia collagen membrane, *Tissue Eng. Part A* 23 (19–20) (2017) 1110–1119.
- [14] N. Nagai, et al., Application of cross-linked salmon atelocollagen to the scaffold of human periodontal ligament cells, *J. Biosci. Bioeng.* 97 (6) (2004) 389–394.
- [15] Z. Lin, et al., Applications of marine collagens in bone tissue engineering, *Biomed. Mater.* 16 (4) (2021) 042007.
- [16] M. López-Álvarez, et al., In vivo evaluation of shark teeth-derived bioapatites, *Clin. Oral Implants Res.* 28 (9) (2017) e91–e100.
- [17] M. López-Álvarez, et al., The improved biological response of shark tooth bioapatites in a comparative in vitro study with synthetic and bovine bone grafts, *Biomed. Mater.* 11 (3) (2016) 035011.
- [18] G.S. Diogo, et al., Marine collagen/apatite composite scaffolds envisaging hard tissue applications, *Mar. Drugs* 16 (8) (2018) 269.
- [19] S.A. Ghodbane, M.G. Dunn, Physical and mechanical properties of cross-linked type I collagen scaffolds derived from bovine, porcine, and ovine tendons, *J. Biomed. Mater. Res. A* 104 (11) (2016) 2685–2692.
- [20] S. Noorzai, et al., Collagen extraction from various waste bovine Hide sources, *Waste Biomass Valoriz.* (2019) 1–12.
- [21] C.G. Sotelo, et al., Characterization of collagen from different discarded fish species of the west coast of the Iberian Peninsula, *J. Aquat. Food Prod. Technol.* 25 (3) (2016) 388–399.
- [22] A.L. Alves, et al., Cosmetic potential of marine fish skin collagen, *Cosmetics* 4 (4) (2017) 39.
- [23] K. Donath, The diagnostic value of the new method for the study of undecalcified bones and teeth with attached soft tissue, (Säge-Schliff, (sawing and grinding) technique), *Pathol. Res. Pract.* 179 (6) (1985) 631–633.
- [24] J. Lackó, L. Géza, A simple differential staining method for semi-thin sections of ossifying cartilage and bone tissues embedded in epoxy resin, *Mikroskopia* 31 (1975) 1–4.
- [25] P. Berillis, Marine collagen: extraction and applications, *Res. Trends Biochem. Mol. Biol. Microbiol.* (2015) 1–13.
- [26] R.O. Sousa, et al., Acid and enzymatic extraction of collagen from Atlantic cod (*Gadus morhua*) swim bladders envisaging health-related applications, *J. Biomater. Sci. Polym. Ed.* 31 (1) (2020) 20–37.
- [27] S. Luca, et al., Marine collagen and its derivatives: versatile and sustainable bio-resources for healthcare, *Mater. Sci. Eng. C* 113 (2020) 1–18, 110963.
- [28] R. Tylingo, et al., Isolation and characterization of acid soluble collagen from the skin of African catfish (*Clarias gariepinus*), salmon (*Salmo salar*) and Baltic cod (*Gadus morhua*), *J. Biotechnol. Biomater.* 6 (234) (2016) 2.
- [29] J. Elango, et al., Evaluation of differentiated bone cells proliferation by blue shark skin collagen via biochemical for bone tissue engineering, *Mar. Drugs* 16 (10) (2018) 350.
- [30] H. Tebyanian, et al., Effects of collagen/ β -tricalcium phosphate bone graft to regenerate bone in critically sized rabbit calvarial defects, *J. Appl. Biomater. Funct. Mater.* 17 (1) (2019) 2280800018820490.
- [31] R.S. Soufdoost, et al., In vitro and in vivo evaluation of novel Tadalafil/ β -TCP/collagen scaffold for bone regeneration: a rabbit critical-size calvarial defect study, *Biocrybern. Biomed. Eng.* 39 (3) (2019) 789–796.
- [32] R.N. Granito, et al., Hydroxyapatite from fish for bone tissue engineering: a promising approach, *Int. J. Mol. Cell. Med.* 7 (2) (2018) 80.
- [33] W. Pon-On, et al., Hydroxyapatite from fish scale for potential use as bone scaffold or regenerative material, *Mater. Sci. Eng. C* 62 (2016) 183–189.

- [34] S. Raynaud, et al., Calcium phosphate apatites with variable Ca/P atomic ratio I. Synthesis, characterisation and thermal stability of powders, *Biomaterials* 23 (4) (2002) 1065–1072.
- [35] H. Cheng, et al., Synergistic interplay between the two major bone minerals, hydroxyapatite and whitlockite nanoparticles, for osteogenic differentiation of mesenchymal stem cells, *Acta Biomater.* 69 (2018) 342–351.
- [36] V. Perez-Puyana, et al., Influence of the processing variables on the microstructure and properties of gelatin-based scaffolds by freeze-drying, *J. Appl. Polym. Sci.* 136 (25) (2019) 47671.
- [37] L. Chen, et al., Synthesis and cytocompatibility of collagen/hydroxyapatite nanocomposite scaffold for bone tissue engineering, *Polym. Compos.* 37 (1) (2016) 81–90.
- [38] M. Ashokkumar, P.M. Ajayan, Materials science perspective of multifunctional materials derived from collagen, *Int. Mater. Rev.* (2020) 1–28.
- [39] K. Lin, et al., Advanced collagen-based biomaterials for regenerative biomedicine, *Adv. Funct. Mater.* 29 (3) (2019) 1804943.
- [40] C.F. Marques, et al., Novel sintering-free scaffolds obtained by additive manufacturing for concurrent bone regeneration and drug delivery: proof of concept, *Mater. Sci. Eng. C* 94 (2019) 426–436.
- [41] S.A. Mosaddad, et al., Fabrication and properties of developed collagen/strontium-doped bioglass scaffolds for bone tissue engineering, *J. Mater. Res. Technol.* 9 (6) (2020) 14799–14817.
- [42] M. Yazdani, et al., Fabrication and properties of β TCP/zeolite/gelatin scaffold as developed scaffold in bone regeneration: in vitro and in vivo studies, *Biocytbern. Biomed. Eng.* 40 (4) (2020) 1626–1637.
- [43] R.A. Perez, G. Mestres, Role of pore size and morphology in musculo-skeletal tissue regeneration, *Mater. Sci. Eng. C* 61 (2016) 922–939.
- [44] K. Sadtlir, et al., Developing a pro-regenerative biomaterial scaffold microenvironment requires T helper 2 cells, *Science* 352 (6283) (2016) 366–370.
- [45] R. Zhang, et al., Effects of the hierarchical macro/mesoporous structure on the osteoblast-like cell response, *J. Biomed. Mater. Res. A* 106 (7) (2018) 1896–1902.
- [46] Q. Zhang, et al., Pore size effect of collagen scaffolds on cartilage regeneration, *Acta Biomater.* 10 (5) (2014) 2005–2013.
- [47] B. Lowe, et al., Preparation and characterization of chitosan-natural nano hydroxyapatite-fucoidan nanocomposites for bone tissue engineering, *Int. J. Biol. Macromol.* 93 (2016) 1479–1487.
- [48] F. Khan, M. Tanaka, Designing smart biomaterials for tissue engineering, *Int. J. Mol. Sci.* 19 (1) (2018) 17.
- [49] D. Coppola, et al., Marine collagen from alternative and sustainable sources: extraction, processing and applications, *Mar. Drugs* 18 (4) (2020) 214.
- [50] J. Enax, et al., Structure, composition, and mechanical properties of shark teeth, *J. Struct. Biol.* 178 (3) (2012) 290–299.
- [51] F. Hao, et al., Assessment of calcium sulfate hemihydrate-tricalcium silicate composite for bone healing in a rabbit femoral condyle model, *Mater. Sci. Eng. C* 88 (2018) 53–60.
- [52] R. Duan, et al., Modulating bone regeneration in rabbit condyle defects with three surface-structured tricalcium phosphate ceramics, *ACS Biomater. Sci. Eng.* 4 (9) (2018) 3347–3355.
- [53] A. Chevrier, et al., Interspecies comparison of subchondral bone properties important for cartilage repair, *J. Orthop. Res.* 33 (1) (2015) 63–70.
- [54] N. Miño-Fariña, et al., Quantitative analysis of the resorption and osteoconduction of a macroporous calcium phosphate bone cement for the repair of a critical size defect in the femoral condyle, *Vet. J.* 179 (2) (2009) 264–272.
- [55] B. Flautre, et al., Porous HA ceramic for bone replacement: role of the pores and interconnections—experimental study in the rabbit, *J. Mater. Sci. Mater. Med.* 12 (8) (2001) 679–682.
- [56] S. Sumathi, B. Gopal, In vitro degradation of multisubstituted hydroxyapatite and fluorapatite in the physiological condition, *J. Cryst. Growth* 422 (2015) 36–43.
- [57] K. Pajor, L. Pajchel, J. Kolmas, Hydroxyapatite and fluorapatite in conservative dentistry and oral implantology—a review, *Materials* 12 (17) (2019) 2683.
- [58] T. Iida, et al., Histological and micro-computed tomography evaluations of newly formed bone after maxillary sinus augmentation using a xenograft with similar density and mineral content of bone: an experimental study in rabbits, *Clin. Exp. Dent. Res.* 4 (6) (2018) 284–290.
- [59] C.L. Chen, et al., A comparison of the bone regeneration and soft-tissue-formation capabilities of various injectable-grafting materials in a rabbit calvarial defect model, *J. Biomed. Mater. Res. B Appl. Biomater.* 107 (3) (2019) 529–544.
- [60] H. Chen, et al., Bone marrow stimulation of the medial femoral condyle produces inferior cartilage and bone repair compared to the trochlea in a rabbit surgical model, *J. Orthop. Res.* 31 (11) (2013) 1757–1764.